murine Jnk1 cDNA. To test c-*jun* and c-*fos* expression, a 199-bp fragment corresponding to nucleotides 891–1,089 of the murine c-*jun* cDNA and a 346-bp fragment corresponding to nucleotides 2,173–2,518 of the murine c-*fos* cDNA were used for the generation of radiolabelled probes for northern hybridization analysis. JNK activity in hippocampal lysates (30 μg) was measured before and after immunodepletion of Jnk1 and Jnk2 by in-gel protein kinase assays using the substrate glutathione *S*-transferase (GST)–cJun[9].

**Luciferase activity assay.** Mice were decapitated and the brains dissected. Brain tissues were immediately lysed (Promega) and the luciferase activity was measured as described[24].

**Kainic acid-induced expression of immediate-early genes.** Homozygous mutant and control wild-type mice were killed and fixed by transcardial perfusion of 4% paraformaldehyde 2 or 6 h after the injection of kainic acid (30 mg per kg, i.p.). Brains from both groups were removed, post-fixed for 1 h, and sectioned on a vibratome (40 μm thick). Tissue sections were processed by immunocytochemistry to detect the expression of c-Jun (Santa Cruz), c-Fos (Santa Cruz), and phosphospecific c-Jun (Ser73) (New England Biolabs). Sections were floated in a solution of the primary antibody (diluted 200×) and incubated overnight at room temperature. Secondary antibody incubation, avidin–biotin conjugated peroxidase (Vectastain Elite ABC kit, Vector) and 3,3′-diaminobenzidine (Sigma) reactions were performed using standard procedures.

**Kainic acid-induced hippocampal damage.** Wild-type and *Jnk3*(–/–) mice were killed and fixed by transcardial perfusion of 4% paraformaldehyde and 1.5% glutaraldehyde 5 days after the injection of kainic acid (30 or 45 mg per kg, i.p.). Semithin and thin sections of brain were prepared using a vibratome and embedded in Epon. Tissue blocks were prepared using a microtome with a diamond tube for 1 μm-thick semithin sections examined by toluidine blue staining and for ultrathin sections examined by electron microscopy. Nissl's stain, GFAP immunocytochemistry, and TUNEL assays were performed using cryostat sections (50 μm) of cerebral hemispheres that were cryoprotected with sucrose. The TUNEL assay was modified from the terminal deoxynucleotidyl transferase (TdT)-mediated dUTP nick end-labelling assay. Briefly, tissue sections, directly mounted on a salinated slide, were permeablized with 2% Triton X-100 (20 min at room temperature) and then incubated for nick end-labelling for 2 h at 37 °C using 0.32 U $\mu l^{-1}$ TdT (Boehringer Mannheim) and 2 μM digoxygenin-11-dUTP (Boehringer Mannheim) in a final volume of 40 μl. The tissues were incubated with anti-digoxygenin antibody (Boehringer Mannheim) at 500× dilution and processed for immunocytochemistry using standard procedures.

Received 11 August; accepted 15 September 1997.


1. Choi, D. W. Glutamate neurotoxicity and diseases of the nervous system. *Neuron* **1,** 623–634 (1988).
2. Coyle, J. T. & Puttfarcken, P. Oxidative stress, glutmate, and neurodegenerative disorders. *Science* **262,** 689–695 (1993).
3. Schwarzschild, M. A., Cole, R. L. & Hyman, S. E. Glutamate, but not dopamine, stimulates stress-activated protein kinase and AP-1-mediated transcription in striatal neurons. *J. Neurosci.* **17,** 3455–3466 (1997).
4. Kawasaki, H. *et al.* Activation and involvement of p38 mitogen-activated protein kinase in glutamate-induced apoptosis in rat cerebellar granule cells. *J. Biol. Chem.* **272,** 18518–18521 (1997).
5. Xia, Z., Dickens, M., Raingeaud, J., Davis, R. J. & Greenberg, M. E. Opposing effects of ERK and JNK-p38 MAP kinases on apoptosis. *Science* **270,** 1326–1331 (1995).
6. Martin, J. H., Mohit, A. A. & Miller, C. A. Developmental expression in the mouse nervous system of the p493F12 SAP kinase. *Brain Res. Mol. Brain Res.* **35,** 47–57 (1996).
7. Gupta, S. *et al.* Selective interaction of JNK protein kinase isoforms with transcription factors. *EMBO J.* **15,** 2760–2770 (1996).
8. Kyriakis, J. M. *et al.* The stress-activated protein kinase subfamily of c-Jun kinases. *Nature* **369,** 156–160 (1994).
9. Derijard, B. *et al.* JNK1: a protein kinase stimulated by UV light and Ha-Ras that binds and phosphorylates the c-Jun activation domain. *Cell* **76,** 1025–1037 (1994).
10. Whitmarsh, A. J. & Davis, R. J. Transcription factor AP-1 regulation by mitogen-activated protein kinase signal transduction pathways. *J. Mol. Med.* **74,** 589–607 (1996).
11. Derijard, B. *et al.* Independent human MAP kinase signal transduction pathways defined by MEK and MKK isoforms. *Science* **267,** 682–685 (1995).
12. Nishina, H. *et al.* Stress-signalling kinase Sek1 protects thymocytes from apoptosis mediated by CD95 and CD3. *Nature* **385,** 350–353 (1997).
13. Sanchez, I. *et al.* Role of SAPK/ERK kinase-1 in the stress-activated pathway regulating transcription factor c-Jun. *Nature* **372,** 794–798 (1994).
14. Yang, D. *et al.* Targeted disruption of the MKK4 gene causes embryonic death, inhibition of JNK activation and defects in AP-1 transcriptional activity. *Proc. Natl Acad. Sci. USA* **94,** 3004–3009 (1997).
15. Tournier, C., Whitmarsh, A. J., Cavanagh, J., Barrett, T. & Davis, R. J. Mitogen-activated protein kinase kinase 7 is an activator of the c-Jun $NH_2$-terminal kinase. *Proc. Natl Acad. Sci. USA* **94,** 7337–7342 (1997).
16. Gupta, S., Campbell, D., Derijard, B. & Davis, R. J. Transcription factor ATF2 regulation by the JNK signal transduction pathway. *Science* **267,** 389–393 (1995).
17. Ben-Ari, Y. Limbic seizure and brain damage produced by kainic acid: mechanisms and relevance to human temporal lobe epilepsy. *Neuroscience* **14,** 375–403 (1985).
18. Ferkany, J. W., Zaczek, R. & Coyle, J. T. The mechanism of kainic acid neurotoxicity. *Nature* **308,** 561–562 (1984).
19. Morgan, J. I. & Curran, T. Stimulus-transcription coupling in the nervous system: involvement of the inducible proto-oncogenes fos and jun. *Annu. Rev. Neurosci.* **14,** 421–451 (1991).
20. Kasof, G. M. *et al.* Kanic acid-induced neuronal death is associated with DNA damage and a unique immediate-early gene response in c-fos-lacZ transgenic rats. *J. Neurosci.* **15,** 4238–4249 (1995).
21. Morgan, J. I., Cohen, D. R., Hempstead, J. L. & Curran, T. Mapping patterns of c-fos expression in the central nervous system after seizure. *Science* **237,** 192–197 (1987).
22. Berger, M. & Ben-Ari, Y. Autoradiographic visualization of [$^3$H]kainic acid receptor subtypes in the rat hippocampus. *Neurosci. Lett.* **39,** 237–242 (1983).
23. Westbrook, G. L. & Lothman, E. W. Cellular and synaptic basis of kainic acid-induced hippocampal epileptiform activity. *Brain Res.* **273,** 97–109 (1983).
24. Rincón, M. & Flavell, R. A. AP-1 transcriptional activity requires both T-cell receptor-mediated and co-stimulatory signals in primary T lymphocytes. *EMBO J.* **13,** 4370–4381 (1994).
25. Rothman, S. M., Thurston, J. H. & Hauhart, R. E. Delayed neurotoxicity of excitatory amino acids in vitro. *Neuroscience* **22,** 471–480 (1987).
26. Bonfoco, E., Krainc, D., Ankarcrona, M., Nicotera, P. & Lipton, S. A. Apoptosis and necrosis: two distinct events induced, respectively, by mild and intense insults with N-methyl-D-aspartate or nitric oxide/superoxide in cortical cell cultures. *Proc. Natl Acad. Sci. USA* **92,** 7162–7166 (1995).
27. Mohit, A. A., Martin, J. H. & Miller, C. A. p493F12 kinase: a novel MAP kinase expressed in a subset of neurons in the human nervous system. *Neuron* **14,** 67–78 (1995).
28. Lipton, S. A. & Rosenberg, P. A. Excitatory amino acids as a final common pathway for neurologic disorders. *N. Engl. J. Med.* **330,** 613–622 (1994).
29. Rothman, S. M. & Olney, J. W. Glutamate and the pathophysiology of hypoxic-ischemic brain damage. *Ann. Neurol.* **19,** 105–111 (1986).
30. Tsirka, S. E., Gualandris, A., Amaral, D. G. & Strickland, S. Excitotoxin-induced neuronal degeneration and seizure are mediated by tissue plasminogen activator. *Nature* **377,** 340–344 (1995).


**Acknowledgements.** This Letter is dedicated to the memory of Morton Nathanson, who suggested key experiments. We thank S. Benzer, D. Y. Loh, C. A. Miller, J. I. Morgan and C. L. Stewart for providing reagents; and T. Barratt, J. Bao, D. Butkis, L. Evangelisti, C. Hughes and J. Musco for technical assistance. R.J.D. and R.A.F. are investigators, and D.D.Y. is an associate, of the Howard Hughes Medical Institute. This work was supported by the Howard Hughes Medical Institute (R.J.D. and R.A.F.) and Public Health Service grants (R.J.D. and P.R.).

Correspondence and requests for materials should be addressed to R.A.F. (e-mail: richard.flavell@qm.yale.edu).

# Identification and characterization of the vesicular GABA transporter

**Steven L. McIntire*‡§, Richard J. Reimer*§, Kim Schuske†§, Robert H. Edwards* & Erik M. Jorgensen†**

* *Graduate Programs in Neuroscience, Cell Biology and Biomedical Sciences, Departments of Neurology and Physiology, UCSF School of Medicine, Third and Parnassus Avenues, San Francisco, California 94143-0435, USA*

† *Department of Biology, University of Utah, 257 South 1400 East, Salt Lake City, Utah 84112-0840, USA*

§ *These authors contributed equally to this work.*

**Synaptic transmission involves the regulated exocytosis of vesicles filled with neurotransmitter. Classical transmitters are synthesized in the cytoplasm, and so must be transported into synaptic vesicles. Although the vesicular transporters for monoamines and acetylcholine have been identified, the proteins responsible for packaging the primary inhibitory and excitatory transmitters, γ-aminobutyric acid (GABA) and glutamate remain unknown[1,2]. Studies in the nematode *Caenorhabditis elegans* have implicated the gene *unc-47* in the release of GABA[3]. Here we show that the sequence of *unc-47* predicts a protein with ten transmembrane domains, that the gene is expressed by GABA neurons, and that the protein colocalizes with synaptic vesicles. Further, a rat homologue of *unc-47* is expressed by central GABA neurons and confers vesicular GABA transport in transfected cells with kinetics and substrate specificity similar to those previously reported for synaptic vesicles from the brain. Comparison of this vesicular GABA transporter (VGAT) with a vesicular transporter for monoamines shows that there are differences in the bioenergetic dependence of transport, and these presumably account for the differences in structure. Thus VGAT is the first of a new family of neurotransmitter transporters.**

‡ Present address: Department of Neurology and the Gallo Center, UCSF, School of Medicine, San Francisco, California 94110, USA.

Studies of synaptic vesicles have identified distinct transport activities for monoamines, acetylcholine (ACh), GABA and glutamate, the classical neurotransmitters. All of these depend on a proton electrochemical gradient $\Delta\mu_{H^+}$ generated by the vacuolar $H^+$-ATPase[1,2]. However, differences in the bioenergetics suggest that the vesicular amino-acid transporters may not belong to the same family of proteins as the vesicular monoamine and ACh transporters. Vesicular monoamine and ACh transport involve the exchange of lumenal protons for cytoplasmic transmitter, and depend primarily on the chemical component ($\Delta$pH) of this gradient. Molecular cloning has also demonstrated that the vesicular monoamine and ACh transporters are closely related in structure[4–6]. In contrast, vesicular glutamate transport depends primarily on the electrical component ($\Delta\Psi$) of $\Delta\mu_{H^+}$, and vesicular GABA transport seems to depend more equally on both $\Delta$pH and $\Delta\Psi$. Attempts to identify additional members of the vesicular monoamine and ACh transporter family, including low-stringency hybridization, polymerase chain reaction (PCR) amplification of the conserved domains using degenerate oligonucleotide primers, and search of the available databases have not yielded additional members (data not shown), suggesting that the sequences encoding vesicular amino-acid transport may be unrelated. Genetic analysis of *C. elegans* provides an alternative means of identifying the sequences responsible for vesicular GABA transport.

We reasoned that mutants lacking GABA transport into vesicles would phenocopy the behaviour of worms in which the GABAergic nervous system had been removed by laser ablation[7]. The 26 GABA-expressing neurons in *C. elegans* are required to inhibit contractions of the head muscles during foraging, to inhibit contractions of the body muscles during locomotion, and to stimulate contraction of the enteric muscles during the defecation cycle[7]. Animals in which the GABAergic neurons are ablated are defective in all three of these

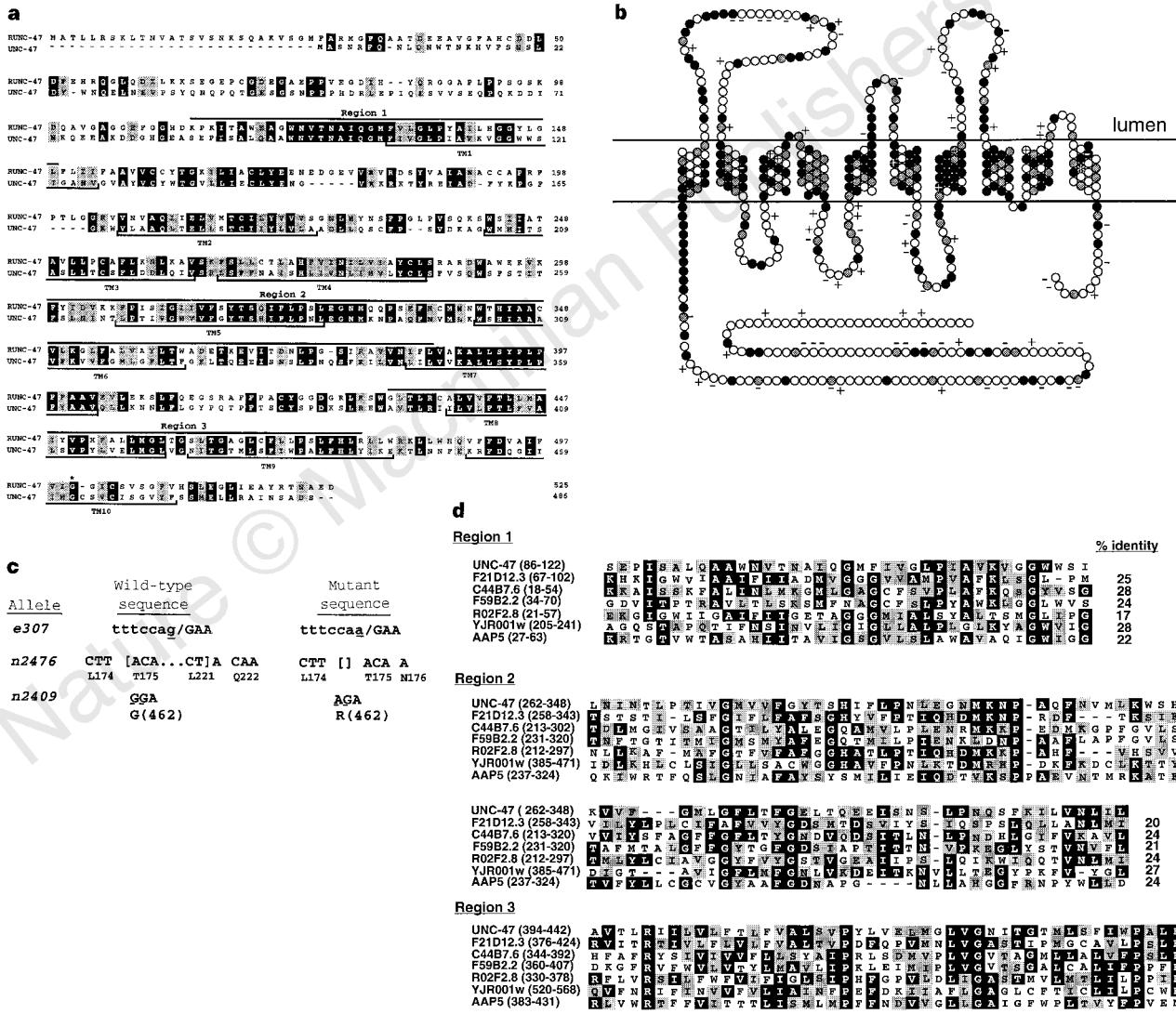


**Figure 1** Sequence and structure of the vesicular GABA transporter. **a**, Alignment of the predicted protein sequence of UNC-47 and the rat UNC-47 homologue (RUNC-47). Predicted transmembrane domains are underlined. Numbers in the right column correspond to amino-acid residues. The conserved amino acid Gly462, which is mutated in allele *n2409*, is indicated with an asterisk. Black boxes indicate identical residues, and grey conservative substitutions. **b**, Predicted secondary structure of rat *unc-47* homologue with the lumen of the vesicle shown above and the cytoplasm below; – represents acidic residues, and + basic residues. Filled circles indicate residues identical (black) or highly conserved (grey) with UNC-47, and open circles indicate divergent residues. Note that the *unc-47* mRNA differs in the first exon from the splice pattern predicted by GeneFinder for T20G5.6. **c**, Mutations in *unc-47*. All mutations were induced by ethyl methanesulphonate (EMS). **d**, UNC-47 defines a new family of polytopic membrane proteins. Comparison of UNC-47 to representative sequences from *C. elegans* (F21D12.3 (U23518), C44B7.6 (U28928), F59B2.2 (P34479), R02F2.8 (U00055)), *S. cerevisiae* (YJR001w (P47082), and plants (amino-acid permease AAP5 (S51170) from *Arabidopsis thaliana*). The comparison shows three colinear regions of highest sequence similarity that are present in all family members. The position of the residues in the sequences of the polypeptides are indicated in parentheses. Residues identical in three or more of the proteins are shown in black and similar residues in grey, as defined by Blast Blossum62 matrix. The % amino-acid identity between UNC-47 and related proteins for each region is shown to the right. The F59B2.2 sequence includes a conserved domain that was present in genomic DNA but was not predicted by GeneFinder.

behaviours. Five genes have been identified that, when mutated, cause defects in these behaviours[3]. However, the phenotype of only one of these mutants, *unc-47*, is consistent with a loss of GABA transport into synaptic vesicles. First, the defect in *unc-47* is global, affecting all of the behaviours mediated by GABA. Second, the defect in *unc-47* is presynaptic, as the muscle cells in the mutant respond normally to GABA receptor agonists[3]. Third, GABA accumulates in GABAergic neurons of the mutant, suggesting that the neurotransmitter is not being released, possibly because it is not loaded into synaptic vesicles.

The *unc-47* gene maps between stP127 and *unc-50* on chromosome III of *C. elegans*. This region contains approximately 250 kilobases (kb) of DNA. Cosmids spanning this region were injected and two cosmid clones, T20G5 and E03F9, each rescued the *unc-47* mutant phenotype. The rescuing activity was further localized to a 5.2-kb *Bam*HI genomic fragment that contains a single complete open reading frame (ORF; T20G5.6) predicted by the *C. elegans* Genome Project[8]. To confirm that the identified ORF corresponds to the gene mutated in *unc-47* worms, three ethyl methanesulphonate-induced alleles were sequenced. The reference allele, *e307* (ref. 9), is a G to A transition of the absolutely conserved G in the splice acceptor site between exons five and six (Fig. 1). A second strong mutation, *n2476*, is a 238-base-pair deletion that removes parts of exons three and four; this deletion causes a frameshift at residue 175 and the ORF terminates after another 115 amino acids, indicating that this allele is a molecular null. Finally, *n2409* is a G to A transition which changes a glycine to arginine at residue 462 in a predicted transmembrane segment.

The cDNA derived from the *unc-47* gene predicts a protein of 486 amino acids (Fig. 1a) with no similarity to the previously characterized vesicular monoamine and ACh transporters[4,6]. However, the sequence predicts ten transmembrane domains (TMDs) consistent with its being involved in transport (Fig. 1b). Further, a search of available databases with the UNC-47 protein sequence revealed that UNC-47 has weak sequence similarity to at least four predicted proteins in *C. elegans*, seven predicted proteins in the yeast *Saccharomyces cerevisiae*, and previously characterized amino-acid permeases in the plants *Arabidopsis thaliana* and *Nicotiana sylvestris* (Fig. 1d), suggesting that UNC-47 belongs to a class of proteins involved in the transport of amino acids.

To identify the cells that express *unc-47*, the protein coding sequence of green fluorescent protein (GFP)[10] was inserted in-frame 52 amino acids downstream of the UNC-47 translation start site and co-injected with a *lin-15*$^+$ (S. G. Clark & X. Lu, personal communication)[11] marker gene into *lin-15(n765ts)* mutant animals[12]. Animals containing the *unc-47*::GFP reporter construct showed expression of GFP in all GABAergic neurons, and only in GABAergic neurons (Fig. 2a), further supporting the idea that *unc-47* is involved in GABA transport.

To determine whether UNC-47 associates with synaptic vesicles, GFP was inserted at the carboxy terminus of the UNC-47 protein. This construct rescued the *unc-47* mutant phenotype, demonstrating that the construct functions normally. GFP-tagged UNC-47 was localized to synaptic varicosities along the ventral and dorsal cords but not in axons (Fig. 2b), a distribution similar to that of other synaptic vesicle proteins such as synaptobrevin[13], synaptotagmin[14], and Rab3a[15]. Further, mislocalization of synaptic vesicles in the *unc-104* mutant (which lacks a neuron-specific kinesin[16]) also results in mislocalization of UNC-47 (Fig. 2c). In *unc-104* mutants, synaptic vesicles do not reach the neuromuscular junction and accumulate in motor-neuron cell bodies[13]. Similarly, in *unc-104* mutants, GFP-tagged UNC-47 is present only in cell bodies and is not transported to the neuromuscular junction (Fig. 2c). Thus the sequence, distribution and subcellular localization of UNC-47 is consistent with its being involved in the packaging of GABA into synaptic vesicles.

To assess the biochemical function of UNC-47, we isolated the cDNA of a vertebrate homologue. A database search with the predicted peptide sequence of *unc-47* identified multiple entries in the mouse expressed sequence tag (EST) database. A fragment of one EST was amplified by PCR and used to screen a mouse brain cDNA library. Partial sequence of a 2.5-kb cDNA showed strong similarity to *unc-47*, and this cDNA was in turn used to screen a rat brain cDNA library. The resulting rat cDNA sequence contains a 3′ untranslated region with ~95% identity to mouse and human but not *C. elegans* sequences (data not shown), a level exceeding that observed in much of the translated domain. The sequence of the largest ORF predicts a protein of 525 amino acids with 38% identity and 56% similarity to *unc-47* (Fig. 1a). Similar to UNC-47, the analysis of hydrophobic moment suggests that there are ten TMDs, and the absence of a single peptide predicts that the amino and the carboxy termini reside in the cytoplasm (Fig. 1b). In addition, the hydrophilic N-terminal domain is unusually large (~132 residues). The hydrophilic loops predicted to reside in the lumen of the vesicle lack consensus sites for N-linked glycosylation. However, consensus sequences for phosphorylation by protein kinase C occur on predicted cytoplasmic domains near the N terminus (+17), between TMDs 2 and 3 (+239) and between TMDs 6 and 7 (+377).

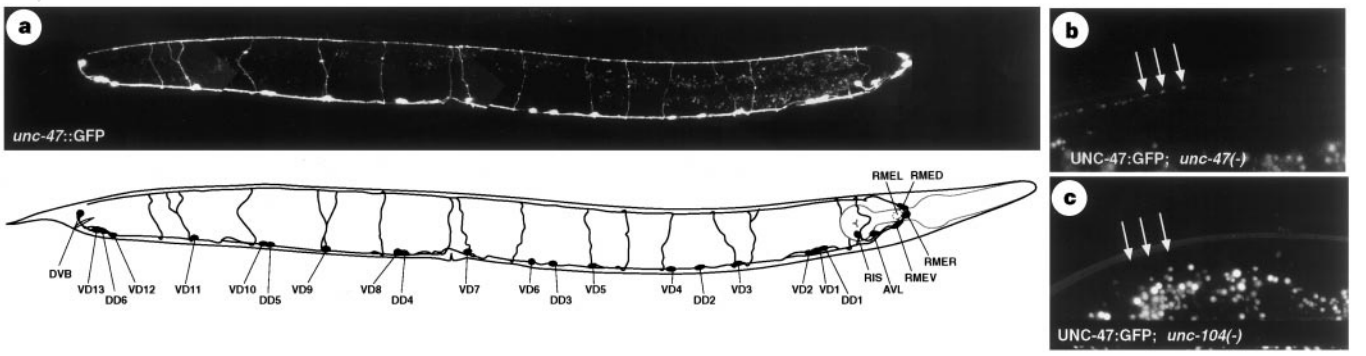


**Figure 2** The *unc-47* gene is transcribed in GABAergic neurons, and the protein colocalizes with synaptic vesicles. **a**, Distribution of neurons that express *unc-47*. A confocal image and camera lucida drawing are shown of an adult *oxIn12* worm, which contains an integrated array of an *unc-47*::GFP reporter construct. GFP is expressed only in the cell bodies and axons of the 26 GABAergic neurons. **b**, Distribution of GFP-tagged UNC-47 protein. An *unc-47(e307)* mutant worm that contains an extrachromosomal array (*oxEx68*) of an UNC-47 GFP translational fusion construct. Confocal image of the dorsal cord at the posterior reflex of the gonad. GFP fluorescence accumulates in synaptic varicosities of the DD motor neurons (arrows). The same distribution of UNC-47:GFP is observed in wild-type animals (not shown). **c**, Colocalization of UNC-47:GFP with synaptic vesicles in *unc-104(e1265)* mutant, which contains an UNC-47:GFP translational fusion construct. GFP is not observed at the nerve terminals of *unc-104* mutants but is only found in the cell bodies. Round spots are autofluorescent gut granules and are not associated with GFP expression.

To determine whether the rat *unc-47* homologue may function presynaptically in GABergic transmission, we examined its tissue distribution. Northern analysis shows expression of an ~2.5 kb mRNA transcript in the brain, with none detected in non-neural tissues (Fig. 3). However, PCR amplification of reverse-transcribed sequences from spleen, testis and pancreas, but not liver or kidney, indicate expression of the *unc-47* homologue (data not shown), consistent with the detection of GABA biosynthesis and transport in some of these tissues[17]. *In situ* hybridization further demonstrates expression of the *unc-47* homologue throughout the neuraxis, but at particularly high levels within the neocortex, hippocampus, cerebellum, striatum, septal nuclei and the reticular nucleus of the thalamus (Fig. 4a–l), regions containing abundant GABAergic neurons. Examination of the autoradiograms under high magnification indicates expression by Purkinje cells of the cerebellum, as well as by interneurons of the cerebellum, hippocampus (Fig. 4m, n) and cortex, which are cell populations known to release GABA. We also performed *in situ* hybridization with one isoform of the biosynthetic enzyme glutamic acid decarboxylase (GAD), GAD-67 (Fig. 4). Although the level of hybridization in different regions varied slightly between the *unc-47* homologue and GAD-67, we found striking colocalization of the two sequences, consistent with the homologue functioning in the release of GABA. We also stained primary hippocampal cultures with an antibody that we raised to the *unc-47* homologue (R.J.R., S.L.M., R.H.E., manuscript in preparation). Punctate immunoreactivity in nerve processes that coincides with the immunoreactivity for synaptophysin is shown in Fig. 4o, p. The apparent vesicular localization further supports the *unc-47* homologue's being involved in vesicular GABA transport.

To determine biochemically whether the rat *unc-47* homologue encodes the vesicular GABA transporter, we expressed the cDNA in rat pheochromocytoma PC12 cells. PC12 cells contain synaptic-like microvesicles and support the activities of the vesicular monoamine transporters[18] as well as the ACh transporter[19], but do not express detectable amounts of *unc-47* homologue (data not shown). Stable PC12 transformants expressing high levels of the putative transport protein were isolated by screening cell clones with antibodies generated against the *unc-47* homologue. Immunofluorescence reveals a punctate pattern that is consistent with localization to intracellular membrane vesicles (data not shown). A population of light vesicles was then isolated from two stable transformants and purified by differential centrifugation. Membranes prepared in this way from the transfected cells show accumulation of $^{3}$H-GABA that is considerably greater than the background uptake observed in membranes from untransfected cells (Fig. 5a). The transport activity present in transfected PC12 cells saturates with increasing concentrations of GABA and has a $K_m$ of ~5 mM (Fig. 5b), consistent with previous observations using rat brain synaptic vesicles[20–23]. Thus the *unc-47* homologue is a vesicular GABA transporter (VGAT).

There are no known potent and specific inhibitors of vesicular GABA transport, so we have characterized in detail the functional

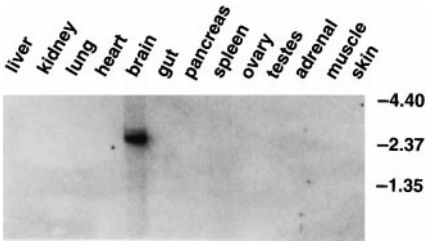


**Figure 3** Brain-specific expression of the rat *unc-47* homologue. Northern analysis of poly(A)$^{+}$ RNA prepared from different tissues shows a 2.5-kb mRNA transcript hybridizing with the rat *unc-47* cDNA only in the brain. The size of standards (kb) are shown on the right.

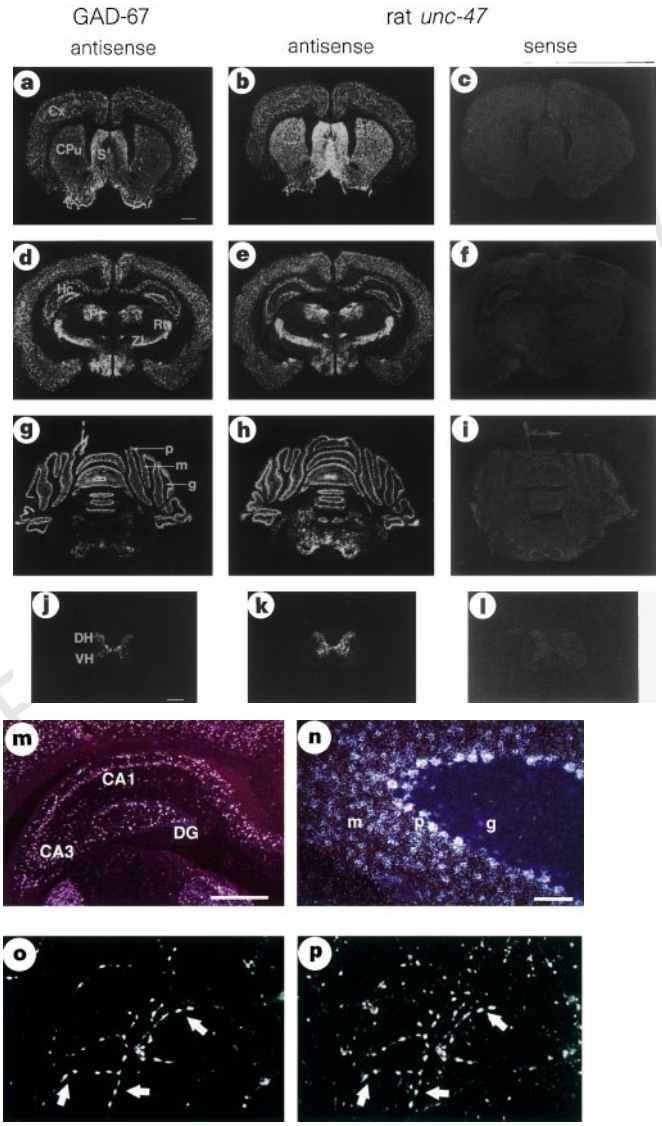


**Figure 4** *In situ* hybridization shows expression of the rat *unc-47* homologue in GABAergic cell populations. **a**–**l**, $^{35}$S-labelled antisense RNA probes for GAD-67 (**a**, **d**, **g**, **j**) and the rat *unc-47* homologue (**b**, **e**, **h**, **k**) and a sense probe for the homologue (**c**, **f**, **i**, **l**) were hybridized with sections through the basal ganglia (**a**–**c**), thalamus (**d**–**f**), cerebellum (**g**–**i**) and spinal cord (**j**–**l**). The pattern of hybridization by the *unc-47* homologue antisense probe appears identical to the antisense probe for GAD67, with no significant hybridization by the sense probes for the *unc-47* homologue or GAD-67 (not shown). Cx, cortex; CPu, caudate-putamen; *S*, septal nuclei; Hc, hippocampus; Pt, pretectal nuclei; Rt, reticular nucleus of the thalamus; ZI, zona incerta; Hy, hypothalamus; p, Purkinje cell layer of the cerebellum; m, molecular layer; g, granule cell layer; DH, dorsal horn of the spinal cord; and VH, ventral horn. Scale bars indicate 1 mm, and the bar in **a** applies to **a**–**i**, the bar in **j** to **j**–**l**. **m**, **n**, Brain sections hybridized with $^{35}$S-labelled antisense RNA for the *unc-47* homologue were counter-stained with cresyl violet and viewed under darkfield illumination. **m**, The hippocampus shows expression in the hilus of the dentate gyrus (DG) and regions CA1 and CA3. Minimal staining occurs in the granule cells of the DG and in pyramidal cells. **n**, The cerebellum shows strong hybridization in the Purkinje cell (p) and molecular layers, with little hybridization in the granule cell layer. Hybridization with the GAD-67 probe shows a similar pattern and sense probes show no signal (data not shown). Scale bars indicate 1 mm (**m**) and 0.1 mm (**n**). **o**, **p**, Double immunofluorescence of primary hippocampal cultures for the *unc-47* homologue (**o**) coincides with immunoreactivity for synaptophysin (**p**). The cells were examined under epifluorescence at ×63 magnification. The arrows indicate processes with coincident staining for both the *unc-47* homologue and synaptophysin. The synaptophysin immunoreactivity that does not correspond to staining for the *unc-47* homologue presumably reflects the presence of non-GABAergic neurons in the culture.

properties encoded by the rat VGAT (rVGAT) cDNA to determine its relationship to the activity previously described in native brain synaptic vesicles. To assess ligand recognition, we first considered compounds structurally related to GABA that have been tested as inhibitors of GABA transport into synaptic vesicles. As for GABA transport into synaptic vesicles, the plasma membrane GABA transport inhibitor nipecotic acid inhibits rVGAT activity only weakly (Fig. 5c), and the excitatory amino-acid transmitter glutamate does not inhibit rVGAT activity even at extremely high concentrations (Table 1)[24–26]. Thus the analysis of ligand specificity also distinguishes rVGAT from these other neurotransmitter transporters. The GABA analogue *N*-butyric acid weakly inhibits both rVGAT activity and GABA transport into brain synaptic vesicles, further supporting the identity of rVGAT as a vesicular GABA transporter. Previous studies using synaptic vesicles have also suggested the inhibition of vesicular GABA transport by γ-vinyl-GABA (vigabatrin), an inhibitor of GABA transaminase and a potent anticonvulsant[27]. This synthetic GABA analogue also inhibits the transport of $^3$H-GABA by rVGAT as potently as unlabelled GABA, supporting the idea that there is an additional site of action for this drug.

Previous studies of native brain synaptic vesicles suggested that a single vesicular GABA transport activity also recognizes the inhibitory amino-acid transmitter glycine as a substrate[23]. However, other studies suggest that glycine has a different transporter[22]. Glycine inhibits GABA transport encoded by the rVGAT cDNA with relatively low potency. We failed to detect significant uptake of $^3$H-glycine in these preparations (data not shown), supporting the existence of a distinct vesicular transporter for glycine.

Functional analysis of rVGAT indicates bioenergetic differences from vesicular transporters for monoamines and ACh. Monamine and ACh transport rely primarily on the chemical component (ΔpH) of the proton electrochemical gradient ($\Delta\mu_{H^+}$)[1,2]. Studies using synaptic vesicles have indicated that vesicular GABA transport relies on the electrical component $\Delta\Psi$, as well as ΔpH[21–23]. To assess the bioenergetics of rVGAT function, we used the ionophore nigericin, which exchanges $K^+$ for $H^+$, to selectively dissipate ΔpH. Nigericin reduces rVGAT activity by ~40%, suggesting that $\Delta\Psi$ has an additional role (Fig. 5d). Indeed, the addition of both nigericin and valinomycin, an ionophore that mediates $K^+$ flux and so dissipates $\Delta\Psi$ as well as ΔpH, eliminates rVGAT activity. To compare directly the bioenergetics of vesicular GABA and monoamine transport, we have examined the transport of serotonin by the same PC12 cell-membrane preparations that contain rVGAT. Previous work has demonstrated the expression of endogenous vesicular monoamine transporter 1 (VMAT1) on synaptic-like microvesicles in these cells[18]. Nigericin inhibits VMAT1 activity on these vesicles to a greater extent (~65%) than it inhibits rVGAT activity, indicating a greater dependence on ΔpH (Fig. 5d). The addition of valinomycin to nigericin eliminates the residual VMAT1

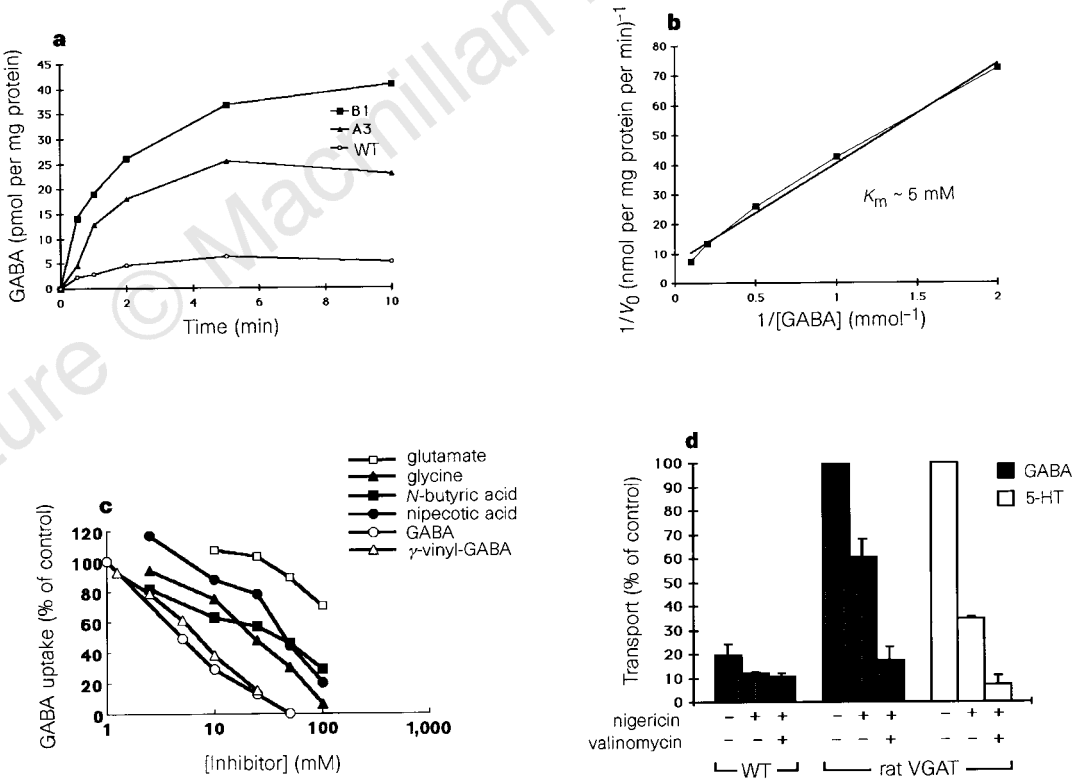


**Figure 5** The rat *unc-47* homologue encodes vesicular GABA transport. **a**, Membranes prepared from two different PC12 cell clones (A3 and B1) stably expressing the rat *unc-47* homologue accumulate more $^3$H-GABA than membranes prepared from untransfected PC12 cells (WT). **b**, Lineweaver–Burke plot of initial, maximal transport rate ($V_0$) in the presence of different concentrations of GABA (μM), with the linear approximation performed by standard regression analysis. **c**, Inhibition of GABA transport activity by GABA and related compounds. γ-Vinyl-GABA inhibits almost as potently as GABA itself, whereas glycine inhibits much less potently and glutamate inhibits only very slightly (see Table 1 for $IC_{50}$ values). *N*-butyric acid and nipecotic acid, an inhibitor of plasma membrane GABA transport, inhibit vesicular GABA transport very weakly. **d**, Vesicular GABA transport and vesicular monoamine transport differ in bioenergetics. Membranes prepared from PC12 cell clone B1 stably expressing rVGAT (middle) show considerably more GABA transport activity (filled bars) than membranes from untransfected cells (WT, left). Nigericin (5 μM) inhibits GABA transport in the transfected cells by ~40%, and the addition of valinomycin (20 μM) to nigericin eliminates rVGAT activity, indicating greater dependence on $\Delta\Psi$ than ΔpH. In contrast, transport of serotonin by endogenous VMAT1 (white bars) expressed in the same membranes from transfected PC12 cells that express rVGAT (right) shows ~65% inhibition by nigericin, indicating that VMAT1 depends more on ΔpH than rVGAT. The results are normalized to GABA transport (left and middle) and serotonin transport (right) by rVGAT-expressing cells. Error bars represent the standard error of the mean.

**Table 1 Inhibition of GABA transport by structurally related compounds**

| Inhibitor | $IC_{50}$ (mM) | s.e. |
|---|---|---|
| GABA | 4.75 | 0.3 |
| γ-Vinyl-GABA | 7.5 | 0.7 |
| Glycine | 27.5 | 10.6 |
| *N*-butyric acid | 43.5 | 2.1 |
| Nipecotic acid | 46 | 1.4 |
| Glutamate | >100 | |

Membranes expressing rVGAT were incubated in 2 μCi $^3$H-GABA for 5 min at 29 °C. The concentrations of structurally related compounds required to inhibit the accumulation of $^3$H-GABA by 50% ($IC_{50}$) are indicated, along with the standard errors (s.e.).

activity, indicating a small role for $\Delta\Psi$. Thus rVGAT and VMAT1 depend on both components of the electrochemical gradient, but VMAT1 depends to a greater extent on ΔpH, which is consistent with previous results using mixed populations of synaptic vesicles.

Identification of the *unc-47* homologue as a vesicular GABA transporter helps us to understand the molecular mechanism for the vesicular transport of an amino-acid neurotransmitter. The genetic analysis in *C. elegans* indicates that *unc-47* is essential for GABA transmission. In addition, UNC-47 and its rat homologue both occur in GABAergic neurons, and their polytopic nature supports the idea that they function in vesicular transport. Biochemical characterization of the rat *unc-47* homologue demonstrates GABA transport function with the affinity and ligand specificity reported for GABA transport by native synaptic vesicles. We cannot detect transport by rVGAT of the other principal inhibitory transmitter glycine, suggesting the existence of a distinct vesicular glycine transporter. The analysis of GABA and monoamine transport activities expressed in the same population of membrane vesicles shows that rVGAT is more dependent on $\Delta\Psi$ than is VMAT1. Indeed, this difference in bioenergetic mechanism may account for the structural differences between these two classes of vesicular transporters. UNC-47 and rVGAT show similarity to a large group of sequences from *C. elegans*, *S. cerevisiae* and plants. Several of the plant sequences mediate amino-acid transport and use a proton electrochemical gradient as the driving force[28], suggesting functional as well as structural similarity to UNC-47 and rVGAT. However, these plant permeases catalyse the co-transport of amino acids and protons rather than the proton exchange mediated by rVGAT, suggesting that the sequence similarity reflects general features of substrate recognition and proton movement, rather than the precise mechanism of bioenergetic coupling. The class of proteins identified by UNC-47 and rVGAT may include the transporters for excitatory amino-acid transmitters, such as glutamate, which also depend on $\Delta\Psi$. □

## Methods

**Cloning of *unc-47*.** A pool containing 10 ng μl$^{-1}$ each of cosmid E03F9, ZK1128, F55E6, T20G5 and K08E5 was injected along with 80 ng μl$^{-1}$ of EK L15 (*lin-15*$^+$) marker plasmid (S. G. Clark & X. Lu, personal communication)[11]. The DNA was injected into the syncytial gonads of *unc-47(e307)*; *lin-15 (n765ts)* animals. Five *lin-15*$^+$ lines were established and all animals were rescued for the *unc-47* mutant phenotypes. A 5.2-kb *Bam*HI fragment subcloned from T20G5 rescued *unc-47(e307)* mutants. The 5.2-kb *Bam*HI fragment was used to screen 350,000 plaques from an oligo-dT-primed λZAP cDNA library made from mixed-stage RNA and a single positive (B1) was identified. To isolate additional cDNAs, 400,000 plaques of a second oligo-dT-primed mixed-stage cDNA library were screened and four positives were isolated (OK1-4). Sequence analysis showed that the B1 cDNA uses an alternative splice donor site in exon five, resulting in deletion of the eighth and part of the ninth TMDs. However, PCR amplification of reverse-transcribed cDNA demonstrated that this mRNA transcript is extremely rare and presumably results from aberrant splicing. The 5′ end of *unc-47* was identified by PCR amplification of first-strand cDNA prepared from mixed-stage poly(A)$^+$ RNA. Sequence analysis of the product revealed an SL1 splice leader immediately 5′ to the ATG start codon. To prepare genomic DNA from mutant alleles *e307*, *n2476*, and *n2409*, approximately 20 homozygous mutant worms were washed three times with M9 salts to remove bacteria, resuspended in 5 μl water, and boiled for 5 min. TE (4 μl), 8.0, and 1 mg ml$^{-1}$ proteinase K (1 μl) were added and the mixture incubated at 45 °C for 1 h. Proteinase K was inactivated by boiling for 30 min, and 1 μl of this DNA preparation was sued for PCR amplification. Amplified fragments were purified and sequenced using the Cyclist *Taq* DNA sequencing kit (Stratagene).

**GFP expression constructs.** To construct the U47GFPNTX transcriptional fusion, GFP and *unc-54* RNA termination sequences were amplified from pPD95.85 (S. Xu & A. Fire, personal communication) using primers that engineered an in-frame *Bsp*HI site onto the 5′ end of GFP. Using an internal *Bsp*HI site, which includes 553 bp of the *unc-54* terminator, the amplified fragment was cloned into the *Bsp*HI site in the *unc-47*-rescuing 5.2-kb *Bam*HI fragment. U47GFPNTX (30 ng μl$^{-1}$) and 35 ng μl$^{-1}$ EK L15 (*lin-15*$^+$) DNA were injected into the gonads of *lin-15(n765ts)* mutants. Three lines carrying an extrachromosomal array of both U47GFPNTX and EK L15 were established, and all three lines expressed GFP in the GABAergic neurons. The extrachromosomal array from one line was integrated into chromosome X by X-ray integration to generate the strain EG1285: *lin-15(n765ts)*; *oxIn12*. To construct the U47GFPCTL translational fusion, a *Sal*I site was engineered into the C terminus of unc-47 protein-coding sequence, two residues N-terminal to the UAA stop codon. GFP was amplified by PCR with primers that engineered an in-frame *Sal*I site onto each end of the GFP fragment and then cloned into the *Sal*I site created at the C terminus of UNC-47. U47GFPCTL (30 ng μl$^{-1}$) and 35 ng μl$^{-1}$ EK L15 (*lin-15*$^+$) DNA were injected into the gonads of *lin-15(n765ts)* and into *lin-15(n765ts)*; *unc-47(e307)* mutant worms, and three *lin-15(n765ts)* lines were established that contained an extrachromosomal array of both U47GFPCTL and *lin-15*$^+$. Four *lin-15(n765ts)*; *unc-47(e307)* lines were obtained that contained both U47GFPCTL and *lin-15*$^+$ in an extrachromosomal array. Worms in two lines had strong GFP expression at the nerve terminals and almost all *lin-15*$^+$ animals were also *unc-47*$^+$. To express U47GFPCTL in the *unc-104(e1265)* mutant background, the *oxEx68* [U47GFPCTL; *lin-15*$^+$] extrachromosomal array was crossed into *unc-104(e1265)*; *lin-15(n765ts)* mutants to generate EG1300: *unc-104*; *lin-15*; *oxEx68*.

**PCR amplification and library screening.** A search of the available EST database with the predicted amino-acid sequence of UNC-47 identified mouse EST 252177 as a possible vertebrate homologue. Using oligonucleotide primers based on 252177, a fragment was amplified by PCR from a pooled mouse brain cDNA library. Briefly, 200 ng template DNA was amplified in a 50-μl reaction containing 25 mM Tris, pH 8.3, 50 mM KCl, 3 mM $MgCl_2$, 100 pmol of each oligonucleotide, 100 μM dNTPs, and 1 μl *Taq* polymerase for 30 cycles involving the denaturation at 92 °C for 1 min, annealing at 66 °C for 1 min, and extension at 72 °C for 1 min. After gel purification, the fragment was radiolabelled by PCR amplification under similar conditions in the presence of 2 μM non-radioactive dCTP and 1 μM $^{32}$P-dCTP and used to screen a mouse brain bacteriophage cDNA library by aqueous hybridization at 47.5 °C (ref. 4). After washing at 52 °C, positively hybridizing phage were identified by autoradiography, purified by two sequential rounds of screening, and the cDNA inserts rescued. After confirmation of the close sequence similarity to *unc-47*, this fragment was radiolabelled by random priming and used to screen a rat brain bacteriophage cDNA library as described above. After characterization of the resulting cDNA clones, the 5′ end of the cDNA was amplified by PCR from a different rat brain cDNA library using oligonucleotide primers from the known rat sequence together with a primer flanking the vector insertion site. Another oligonucleotide primer based on the additional sequence was then used to amplify the 5′ end of the cDNA from the library with *Pfu* polymerase rather than *Taq* polymerase to minimize mutations. This 5′ fragment was then joined to a cDNA clone isolated by hybridization at a common *Bgl*II restriction site. The dideoxy chain termination method was used to confirm the sequence of the cDNA on both strands.

**Northern analysis.** Poly(A)$^+$ RNA (5 μg) prepared from different rat tissues was separated by electrophoresis through formaldehyde–agarose and transferred to nylon membranes. Staining with ethidium bromide revealed approximately equal amounts of RNA in each lane. After hybridization in 50% formamide[4] to the *unc-47* homologue cDNA radiolabelled by random priming, the filters were autoradiographed with an enhancing screen.

***In situ* hybridization.** Adult rats were anaesthetized with pentobarbital and perfused with 4% paraformaldehyde in phosphate-buffered saline (PBS). After dissection, the brains were postfixed in the same solution, cryoprotected in

30% sucrose/PBS, and 15-μm sections hybridized at 52 °C in 50% formamide containing 0.3 M NaCl, 20 mM Tris, pH 7.4, 5 mM EDTA, 10 mM $NaH_2PO_4$, 1× Denhardt's solution, 10% dextran sulphate, and 0.5 mg $ml^{-1}$ yeast RNA to $^{35}$S-labelled RNA probes transcribed from linearized plasmid templates and hydrolysed in alkali to ~300 nucleotide fragments[29]. After washes in 50% formamide and digestion with RNase A, the slides were autoradiographed.

**Immunofluorescence.** Primary hippocampal cultures were grown on poly-D-lysine-coated glass coverslips for two weeks, fixed in 4% paraformaldehyde/PBS for 20 min, rinsed in PBS, blocked in 0.02% saponin, 2% BSA, 1% fish skin gelatin/PBS (blocking buffer) for 1 h and incubated for 90 min with anti-rVGAT polyclonal rabbit and anti-synaptophysin monoclonal mouse antibodies diluted 1 : 100 in blocking buffer, all at room temperature. The cells were then washed, incubated in secondary anti-rabbit antibody conjugated to fluorescein and anti-mouse antibody conjugated to rhodamine (both Cappel) both diluted 1 : 100, washed, the coverslips mounted on class slides, and viewed under epifluorescence.

**Membrane preparation.** The rat *unc-47* homologue cDNA subcloned into the plasmid expression vector pcDNA3-Amp (Invitrogen) was introduced into PC12 cells by electroporation[30]. The cells were then selected in 800 μg $ml^{-1}$ G418 (effective) and the resulting clones examined by immunofluorescence[18] using a rabbit polyclonal antibody (R.R., S.M. & R.H.E., manuscript in preparation). Using the two cell clones with the highest level of immunoreactivity, membranes were prepared by first resuspending the washed cells in 0.3 M sucrose, 10 mM HEPES-KOH, pH 7.4 (SH buffer) containing 0.2 mM diisopropylfluorophosphate (DFP), 1 μg $ml^{-1}$ pepstatin, 2 μg $ml^{-1}$ aprotinin, 2 μg $ml^{-1}$ leupeptin, 1 μg $ml^{-1}$ E64 and 1.25 mM MgEGTA. The cells were then disrupted by homogenization at 4 °C through a ball-bearing device at a clearance of 10 μm. The nuclear debris was sedimented at 1,000*g* for 5 min and heavier membranes were eliminated by centrifugation at 27,000*g* for 1 h. The remaining light membrane vesicles were sedimented at 65,000*g* for 1 h and resuspended in SH containing the same protease inhibitors at a final concentration of ~10 μg protein per μl.

**Transport assay.** To initiate the reaction, 10 μl of membranes was added to 200 μl SH buffer containing 4 mM $MgCl_2$, 4 mM KCl, 4 mM ATP, 40 μM unlabelled GABA and 2 μCi $^3$H-GABA (NEN). Incubation was performed at 29 °C for varying intervals and the reaction was terminated by rapid filtration (Supor 200, Gelman), followed by immediate washing with 6 ml cold 0.15 M KCl. Background uptake was determined by incubation at 4 °C for 0 min. The bound radioactivity was measured by scintillation counting in 2.5 ml Cytoscint (ICN). To determine $K_m$, unlabelled GABA was added at a range of concentrations and uptake were measured at 30 s. Nigericin and valinomycin dissolved in ethanol added to final concentrations of 5 μM and 20 μM, respectively. Transport measurements were performed in duplicate and repeated three or more times using at least two different membrane preparations.

Received 18 July; accepted 29 September 1997.


1. Schuldiner, S., Shirvan, A. & Linial, M. Vesicular neurotransmitter transporters: from bacteria to humans. *Physiol. Rev.* **75,** 369–392 (1995).
2. Liu, Y. & Edwards, R. H. The role of vesicular transport proteins in synaptic transmission and neural degeneration. *Annu. Rev. Neurosci.* **20,** 125–156 (1997).
3. McIntire, S., Jorgensen, E. & Horvitz, H. R. Genes required for GABA function in *Caenorhabditis elegans*. *Nature* **364,** 337–341 (1993).
4. Liu, Y. *et al.* A cDNA that supresses MPP+ toxicity encodes a vesicular amine transporter. *Cell* **70,** 539–551 (1992).
5. Erickson, J. D., Eiden, L. E. & Hoffman, B. J. Expression cloning of a reserpine-sensitive vesicular monoamine transporter. *Proc. Natl Acad. Sci. USA* **89,** 10993–10997 (1992).
6. Alfonso, A., Grundahl, K., Duerr, J. S., Han, H.-P. & Rand, J. B. The *Caenorhabditis elegans unc-17* gene: a putative vesicular acetylcholine transporter. *Science* **261,** 617–619 (1993).
7. McIntire, S., Jorgensen, E., Kaplan, J. & Horvitz, H. R. The GABAergic nervous system of *Caenorhabditis elegans*. *Nature* **364,** 334–337 (1993).
8. Wilson, R. *et al.* 2.2 Mb of contiguous nucleotide sequence from chromosome III of *C. elegans*. *Nature* **368,** 32–38 (1994).
9. Brenner, S. The genetics of *Caenorhabditis elegans*. *Genetics* **77,** 71–94 (1974).
10. Chalfie, M., Tu, Y., Euskirchen, G., Ward, W. W. & Prasher, D. C. Green fluorescent protein as a marker for gene expression. *Science* **263,** 802–805 (1994).
11. Clark, S. G., Lu, X. & Horvitz, H. R. The *Caenorhabiditis elegans* locus *lin-15*, a negative regulator of a tyrosine kinase signaling pathway, encodes two different proteins. *Genetics* **137,** 987–997 (1994).
12. Ferguson, E. L. & Horvitz, H. R. Identification and characterization of 22 genes that affect the vulval cell lineages of the nematode *Caenorhabidits elegans*. *Genetics* **110,** 17–72 (1985).
13. Jorgensen, E. M. *et al.* Defective recycling of synaptic vesicles in synaptotagmin mutants of *Caenorhabditis elegans*. *Nature* **378,** 196–199 (1995).
14. Nonet, M. L., Grundahl, K., Meyer, B. J. & Rand, J. B. Synaptic function is impaired but not eliminated in *C. elegans* mutants lacking synaptotagmin. *Cell* **73,** 1291–1306 (1993).
15. Nonet, M. L. *et al.* Functional synapses are partially depleted of vesicles in *C. elegans rab-3* mutants. *J. Neurosci.* (in the press).
16. Hall, D. H. & Hedgecock, E. M. Kinesin-related gene *unc-104* is required for axonal transport of synaptic vesicles in *C. elegans*. *Cell* **65,** 837–847 (1991).
17. Thomas-Reetz, A. *et al.* γ-aminobutyric acid transporter driven by a proton pump is present in synaptic-like microvesicles of pancreatic B cells. *Proc. Natl Acad. Sci. USA* **90,** 5317–5321 (1993).
18. Liu, Y. *et al.* Preferential localization of a vesicular monoamine transporter to dense core vesicle in PC12 cells. *J. Cell Biol.* **127,** 1419–1433 (1994).
19. Varoqui, H. & Erickson, J. D. Active transport of acetylcholine by the human vesicular acetylcholine transporter. *J. Biol. Chem.* **271,** 27229–27232 (1996).
20. Fykse, E. M. & Fonnum, F. Uptake of γ-aminobutyric acid by a synaptic vesicle fraction isolated from rat brain. *J. Neurochem.* **50,** 1237–1242 (1988).
21. Hell, J. W., Maycox, P. R., Stadler, H. & Jahn, R. Uptake of GABA by rat brain synaptic vesicles isolated by a new procedure. *EMBO J.* **7,** 3023–3029 (1988).
22. Kish, P. E., Fischer-Bovenkerk, C. & Ueda, T. Active transport of γ-aminobutyric acid and glycine into synaptic vesicles. *Proc. Natl Acad. Sci. USA* **86,** 3877–3881 (1989).
23. Burger, P. M. *et al.* GABA and glycine in synaptic vesicles: storage and transport characteristics. *Neuron* **7,** 287–293 (1991).
24. Naito, S. & Ueda, T. Adenosine triphosphate-dependent uptake of glutamate into protein I-associated synaptic vesicles. *J. Biol. Chem.* **258,** 696–699 (1983).
25. Maycox, P. R., Deckwerth, T., Hell, J. W. & John, R. Glutamate uptake by brain synaptic vesicles. Energy dependence of transport and functional reconstitution in proteoliposomes. *J. Biol. Chem.* **263,** 15423–15428 (1988).
26. Carlson, M. D., Kish, P. E. & Ueda, T. Glutamate uptake into synaptic vesicles: competitive inhibition by bromocriptine. *J. Neurochem.* **53,** 1889–1894 (1989).
27. Christensen, H., Fykse, E. M. & Fonnum, F. Inhibition of γ-aminobutyrate and glycine uptake into synaptic vesicles. *Eur. J. Pharmacol.* **207,** 73–79 (1991).
28. Fischer, W. N., Kwart, M., Hummel, S. & Frommer, W. B. Substrate specificity and expression of profile of amino acid transporters (AAPs) in *Arabidopsis*. *J. Biol. Chem.* **270,** 16315–16320 (1995).
29. Sassoon, D. & Rosenthal, N. in *Guide to Techniques in Mouse Development* (eds Wassarman, P. M. & DePamphilis, M. L.) 384–404 (Academic, San Diego, 1993).
30. Grote, E., Hao, J. C., Bennett, M. K. & Kelly, R. B. A targeting signal in VAMP regulating transport ot synaptic vesicles. *Cell* **81,** 581–589 (1995).


**Acknowledgements.** We thank B. Westlund for unpublished *unc-47* map data; E. King for help with the confocal microscope; H. Rausch and K. Knobel for integrating the *unc-47*::GFP transcriptional fusion construct; Y. Jin for the *n2476* allele; D. P. Morse and B. Bamber for the gift of RNA and cDNA; R. Barstead and P. Okkema for the *C. elegans* cDNA libraries; J. Boulter and D. Julius for the mammalian cDNA libraries; D. Rice and D. Eisenberg for the analysis of hydrophobic moment; A. Tobin and S. Baekkeskov for the GAD-67 cDNA; Y. Liu and P. Tan for assistance in the isolation of PC12 cell clones and the preparation of membranes; J. Hell and P. Finn for suggestions about the measurement of transport activity; S. Craven and D. Bredt for assistance with the primary hippocampal cultures; and M. Horner, E. Kofoid, C. Bargmann and members of the Edwards and Jorgensen laboratories for discussions. This work was supported by the Gallo Center (S.L.M.), the Giannini Foundation (R.J.R.), an NIH Developmental Biology training grant (K.S.), the Klingenstein Foundation (E.M.J.), NINDS (S.L.M., R.H.E., E.M.J.) and NIMH (R.H.E.).

Correspondence and requests for materials should be addressed to R.H.E. (e-mail: edwards@itsa.ucsf.edu) or E.M.J. (e-mail: jorgensen@bioscience.biology.utah.edu).

# Activation of the transcription factor Gli1 and the Sonic hedgehog signalling pathway in skin tumours

**N. Dahmane*, J. Lee*, P. Robins†, P. Heller† & A. Ruiz i Altaba***

* *The Skirball Institute, Developmental Genetics Program and Department of Cell Biology, and † Department of Dermatology, New York University Medical Center, 540 First Avenue, New York, New York 10016, USA*

**Sporadic basal cell carcinoma (BCC) is the most common type of malignant cancer in fair-skinned adults. Familial BCCs and a fraction of sporadic BCCs have lost the function of Patched (Ptc), a Sonic hedgehog (Shh) receptor[1–3] that acts negatively on this signalling pathway. Overexpression of Shh can induce BCCs in mice[4]. Here we show that ectopic expression of the zinc-finger transcription factor Gli1 in the embryonic frog epidermis results in the development of tumours that express endogenous *Gli1*. We also show that *Shh* and the *Gli* genes are normally expressed in hair follicles, and that human sporadic BCCs consistently express *Gli1* but not *Shh* or *Gli3*. Because Gli1, but not Gli3, acts as a target and mediator of Shh signalling[5], our results suggest that expression of Gli1 in basal cells induces BCC formation. Moreover, loss of Ptc or overexpression of Shh cannot be the sole causes of Gli1 induction and sporadic BCC formation, as they do not occur consistently. Thus any mutations leading to the expression of Gli1 in basal cells are predicted to induce BCC formation.**

*Gli1*, which was originally isolated as an amplified gene in a glioma[6], is a member of a multigene family[7–9] and can transform